Vascular Pharmacology 117 (2019) 15–26

Contents lists available at ScienceDirect

Vascular Pharmacology

journal homepage: www.elsevier.com/locate/vph

Asiatic acid stabilizes cytoskeletal proteins and prevents TNF-α-induced disorganization of cell-cell junctions in human aortic endothelial cells

Lai Yen Fong[a,c,*], Chin Theng Ng[a,d], Yoke Keong Yong[b], Muhammad Nazrul Hakim[a], Zuraini Ahmad[a]

[a] Department of Biomedical Science, Faculty of Medicine and Health Sciences, Universiti Putra Malaysia, 43400 Serdang, Selangor, Malaysia
[b] Department of Human Anatomy, Faculty of Medicine and Health Sciences, Universiti Putra Malaysia, 43400 Serdang, Selangor, Malaysia
[c] Department of Pre-clinical Sciences, Faculty of Medicine and Health Sciences, Universiti Tunku Abdul Rahman, 43000 Kajang, Selangor, Malaysia
[d] Physiology Unit, Faculty of Medicine, AIMST University, 08100 Bedong, Kedah, Malaysia

ARTICLE INFO

Keywords:
TNF-α
Asiatic acid
Anti-hyperpermeability
Actin
Diphosphorylated myosin light chain
Endothelial cell-cell junctions
Human aortic endothelial cells

ABSTRACT

Endothelial hyperpermeability represents an initiating step in early atherosclerosis and it often occurs as a result of endothelial barrier dysfunction. Asiatic acid, a major triterpene isolated from *Centella asiatica* (L.) Urban, has previously been demonstrated to protect against tumor necrosis factor (TNF)-α-induced endothelial barrier dysfunction. The present study aimed to investigate the mechanisms underlying the barrier protective effect of asiatic acid in human aortic endothelial cells (HAECs). The localization of F-actin, diphosphorylated myosin light chain (diphospho-MLC), adherens junctions (AJs) and tight junctions (TJs) was studied using immunocytochemistry techniques and confocal microscopy. Their total protein expressions were examined using western blot analysis. The endothelial permeability was assessed using *In Vitro* Vascular Permeability Assay kits. In addition, intracellular redistribution of the junctional proteins was evaluated using subcellular fractionation kits. We show that asiatic acid stabilized F-actin and diphospho-MLC at the cell periphery and prevented their rearrangement stimulated by TNF-α. However, asiatic acid failed to attenuate cytochalasin D-induced increased permeability. Besides, asiatic acid abrogated TNF-α-induced structural reorganization of vascular endothelial (VE)-cadherin and β-catenin by preserving their reticulum structures at cell-cell contact areas. In addition, asiatic acid also inhibited TNF-α-induced redistribution of occludin and zona occludens (ZO)-1 in different subcellular fractions. In conclusion, the barrier-stabilizing effect of asiatic acid might be associated with preservation of AJs and prevention of TJ redistribution caused by TNF-α. This study provides evidence to support the potential use of asiatic acid in the prevention of early atherosclerosis, which is initiated by endothelial barrier dysfunction.

1. Introduction

Atherosclerosis is a chronic inflammatory disease which is closely associated with endothelial cell activation at the early stage. One of the hallmarks of endothelial cell activation is increased endothelial permeability, which can be triggered by various pro-atherogenic stimuli including low density lipoprotein (LDL), mechanical forces and cytokines such as tumor necrosis factor (TNF)-α and interferon (IFN)-γ [1]. In physiological conditions, the endothelium maintains endothelial permeability by selectively allowing the passage of solutes and small molecules, while restricting extravasation of large molecules and blood cells. An increase in endothelial permeability permits the entry of LDL into the intima and become oxidized, which in turn initiates atherogenesis [2]. Therefore, therapeutic approaches targeting endothelial barrier dysfunction may represent a promising strategy to hinder the onset of early pre-lesional atherosclerotic events.

Both adherens junctions (AJs) and tight junctions (TJs) connect neighboring endothelial cells through homophilic interactions and hence, play crucial roles in the regulation of endothelial permeability. VE-cadherin and adaptor proteins such as α-, β- and p120-catenin form

Abbreviations: diphospho-MLC, diphosphorylated myosin light chain; AJs, adherens junctions; TJs, tight junctions; HAECs, human aortic endothelial cells; TTFCA, total triterpenic fraction of Asian *C. asiatica*; TNF-α, tumor necrosis factor- α; IFN- γ, interferon-γ; VE-cadherin, vascular endothelial cadherin; ZO-1, zona occludens 1; G-actin, globular actin; F- actin, filamentous actin; FITC-dextran, fluorescein isothiocyanate-conjugated dextran

* Corresponding author at: Department of Pre-clinical Sciences, Faculty of Medicine and Health Sciences, Universiti Tunku Abdul Rahman, 43000 Kajang, Selangor, Malaysia.
E-mail address: fongly@utar.edu.my (L.Y. Fong).

https://doi.org/10.1016/j.vph.2018.08.005
Received 4 May 2018; Received in revised form 12 July 2018; Accepted 11 August 2018
Available online 13 August 2018
1537-1891/

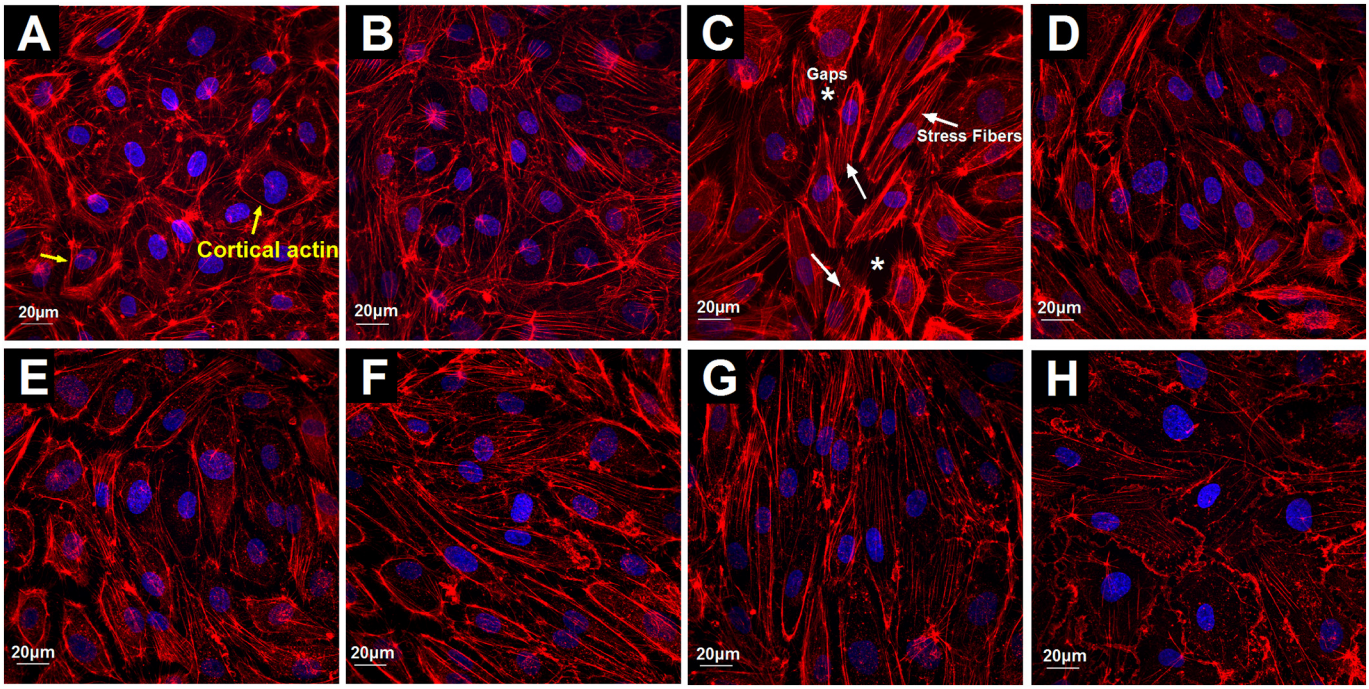

Fig. 1. Asiatic acid partially attenuates TNF-α-induced F-actin rearrangement. (A-H) Representative confocal images showing F-actin distribution. (A) Non-stimulated HAECs possessed thick cortical actin ring (*yellow arrows*) along the cell borders. (B) The cells treated with 40 μM of asiatic acid alone. (C) TNF-α caused stress fiber formation (*white arrows*), appearance of intercellular gaps (*asterisks*) and cell elongation. (D) 10 μM and (E) 20 μM of asiatic acid pretreatement did not prevent TNF-α-induced F-actin rearrangement. The cells pretreated with asiatic acid at (F) 30 μM and (G) 40 μM showed prominent F-actin localization at the cell periphery, while a few stress fibers were being observed at the end of cell margin. (H) The cells pretreated with simvastatin for 24 h. Red colour represents F-actin and blue colour represents nuclei. (Bar = 20 μm). (For interpretation of the references to colour in this figure legend, the reader is referred to the web version of this article.)

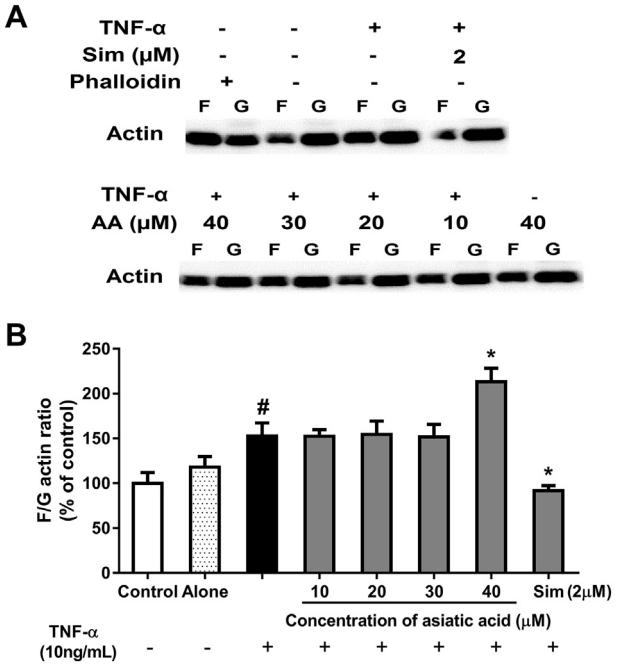

Fig. 2. Asiatic acid augments TNF-α-induced increased F/G-actin ratio. (A) Representative blots showing F- and G-actin concentrations. (B) Densitometry analysis for the amount of F- and G-actin. Results are expressed as mean ± SEM. The control F/G ratio is 100 ± 11.9%. AA, asiatic acid; Alone, 40 μM of asiatic acid alone; Sim, simvastatin. # indicates $p < 0.05$ compared to control; * indicates $p < 0.05$ compared to TNF-α-stimulated group.

AJ complexes while occludin and claudins link to their respective adaptor protein, zona occludens (ZO)-1, and form TJ complexes. The adaptor proteins provide a linkage between intercellular junctions and the intracellular cytoskeleton. Alterations in the assembly of the cytoskeleton thus, affect the junction stability and cause the endothelial barrier to disrupt [3]. In physiological conditions, cytoskeletal proteins such as actin undergo continuous remodeling to control cell motility, contraction and permeability [4]. Actin organize themselves into either a monomer form known as globular (G)-actin or a polymer form known as filamentous (F-)-actin. Furthermore, the dynamic of actin is well known to be mediated by myosin light chain (MLC). Phosphorylation of MLC has been reported to cause F-actin reorganization and stress fiber formation, thereby increasing cell contraction and endothelial permeability [5].

Centella asiatica is a medicinal herb commonly found in tropical regions such as Asia (Sri Lanka, China, India and Malaysia), Africa, South America and Oceania. Apart from its medicinal properties, the Southeast Asian usually consume *C. asiatica* as salads in daily meals or serve it as thirst quenching juices [6]. In Europe, total triterpenic fraction of Asian *C. asiatica* (TTFCA) is marketed under various trade names such as Madecassol®, Centellase® and Blastoestimulina and is mainly used for the treatment of wounds and chronic venous insufficiency [7].

Clinical studies have shown that TTFCA stabilizes arterial plaques in patients [8, 9]. Recently, researchers reported that a nutritional supplement containing TTFCA possesses anti-atherosclerotic effects in asymptomatic patients and it is associated with a reduction of oxidative stress [10–12]. Besides, TTFCA has also been demonstrated to improve permeability of the microcirculation and prevent tissue edema in hypertensive patients [13, 14]. Besides than these significant clinical data, studies intended to investigate the anti-atherosclerotic effects of *C. asiatica* using animal and cell culture models remain widely lacking. Hence, detailed mechanistic study is needed in order to support the potential use of *C. asiatica* as an anti-atherogenic agent.

Asiatic acid, a major pentacyclic triterpenoid isolated from *C. asiatica*, has been reported to possess anti-hyperlipidemic [15], anti-inflammatory [16, 17], anti-oxidant [18], anti-diabetic [19] and anti-

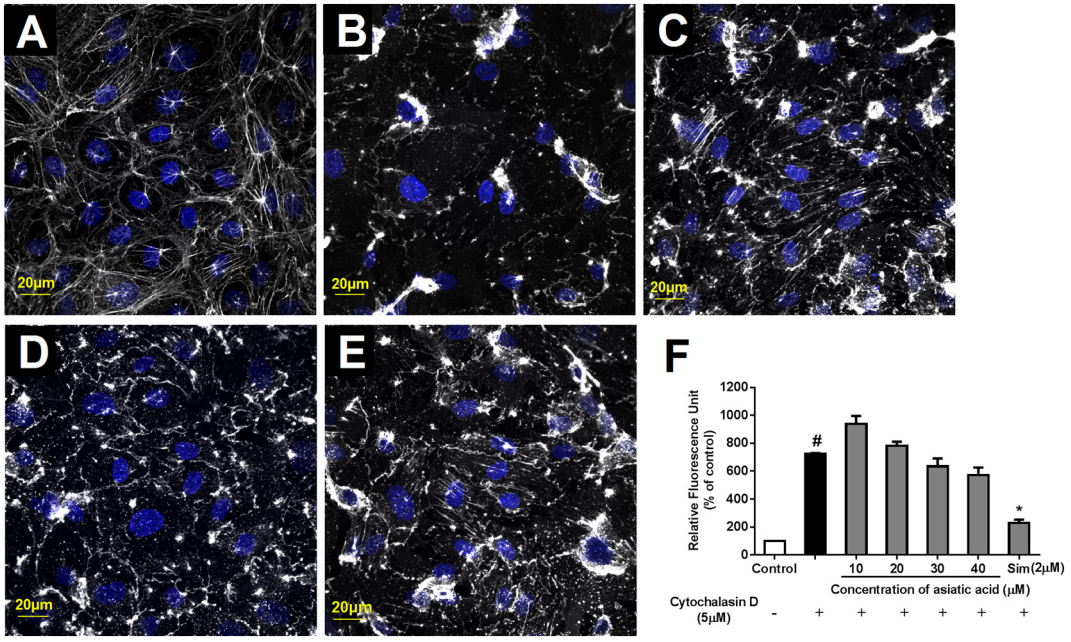

Fig. 3. Asiatic acid attenuates cytochalasin D-induced F-actin disruption by stabilizing peripheral F-actin filaments but does not reduce cytochalasin D-induced increased permeability. (A–E) Representative confocal images showing F-actin distribution. HAECs were treated with asiatic acid for 6 h before incubated with 5 μM of cytochalasin D for 15 min. (A) Control HAECs possessed thick cortical actin ring. (B) Cytochalasin D disrupted F-actin organization and condensed the F-actin staining around the perinucelar regions. (C) 20 μM, (D) 30 μM and (E) 40 μM of asiatic acid stabilizes peripheral F-actin filaments upon cytochalasin D disruption. Three independent experiments were performed. White colour represents F-actin and blue colour represents nuclei. (F) HAECs were treated with asiatic acid for 6 h before induced with 5 μM of cytochalasin D for 15 min. The passage of FITC-dextran was measured as relative fluorescence unit by collecting media from the bottom chamber at the end of the experiment. Data are expressed as mean ± SEM of three independent experiments. Sim, simvastatin. # indicates $p < 0.05$ compared to control; * indicates $p < 0.05$ compared to cytochalasin D-induced group. (For interpretation of the references to colour in this figure legend, the reader is referred to the web version of this article.)

hypertensive [20, 21] activities. We have previously demonstrated that asiatic acid inhibits TNF-α-induced endothelial hyperpermeability in human aortic endothelial cells (HAECs) [22]. This study aimed to investigate the mechanism underlying the barrier protective effect of asiatic acid, where effects of asiatic acid on F-actin, diphosphorylated MLC (diphospho-MLC), AJs and TJs in the presence of TNF-α were examined.

2. Materials and methods

2.1. Materials

Asiatic acid isolated from *C. asiatica* with a purity of 93% was purchased from Chromadex (CA, USA). Human recombinant TNF-α was purchased from Peprotech (NJ, USA). 22 mm BD Biocoat collagen-coated German glass coverslips was purchased from BD Biosciences (CA, USA). Rhodamine-conjugated phalloidin, Prolong Gold anti fade agent, rabbit polyclonal anti-ZO-1, rabbit polyclonal anti-occludin and Alexa Fluor 488-conjugated goat anti-rabbit IgG secondary antibody were purchased from Molecular Probes (OR, USA). Rabbit polyclonal anti-phospho-MLC 2 (Thr18/Ser19), rabbit polyclonal anti-VE-cadherin, rabbit polyclonal anti-β-catenin, horseradish peroxidase (HRP)-linked anti-rabbit IgG, HRP-conjugated rabbit monoclonal anti-β-actin were purchased from Cell Signaling Technology (MA, USA). Cytochalasin D was purchased from Sigma (MO, USA).

2.2. Cell culture

Primary HAECs were purchased from American Type Cell Culture (ATCC) and maintained in endothelial cell medium (Sciencell, CA, USA) supplemented with 5% fetal bovine serum, 100 U/mL penicillin, 100 μg/mL streptomycin and endothelial cell growth supplements at 37 °C and 5% CO_2. Cells under passage 5 were used for all the experiments. In all experiments, HAECs were pre-treated with 10–40 μM of asiatic acid for 6 h before the cells were induced with 10 ng/mL of TNF-α for another 6 h, unless otherwise specified.

2.3. F-actin staining

F-actin filaments were stained using rhodamine-conjugated phalloidin according to the manufacturer's protocols. HAECs were seeded onto 22 mm collagen-coated coverslips (3×10^5 cells per coverslip) and allowed to grow for 4–6 days to reach confluence. After the indicated treatment period, the cells were fixed with 3.7% formaldehyde for 10 min. Then, the cells were washed and permeabilized with 0.1% Triton X-100 for 5 min. Each coverslip was stained with rhodamine phalloidin (5 μL of methanol stock solution in 200 μL of PBS) for 20 min and mounted with ProLong Gold anti-fade agent. 5 fields per coverslip were randomly captured using a confocal laser scanning microscope (FV1000, Olympus, Tokyo, Japan). *Z*-stack was performed over an average depth of 4 μm and 9–11 Z-stack were collected for each field. All single sections were then compiled into a single image.

2.4. Quantification of F/G actin ratio

The cellular fractions containing F and G-actin were separated using G/F actin *In vivo* assay kit (Cytoskeleton, CO, USA) according to the manufacturer's protocol. HAECs were grown onto 6-well plates (1×10^5 cells/well). After treatment, the cells were lysed in 100 μL of a warm lysis buffer containing F-actin stabilization buffer, adenosine triphosphate (ATP) and protease inhibitor cocktail. The lysates were homogenized several times before they were incubated at 37 °C for 10 min. After a short spin, the supernatant was collected and centrifuged at 100,000 × *g* for 1 h in order to separate the G-actin and F-actin fractions. After centrifugation, the supernatant sample was kept as G-actin fraction. 100 μL of F-actin depolymerization buffer was added

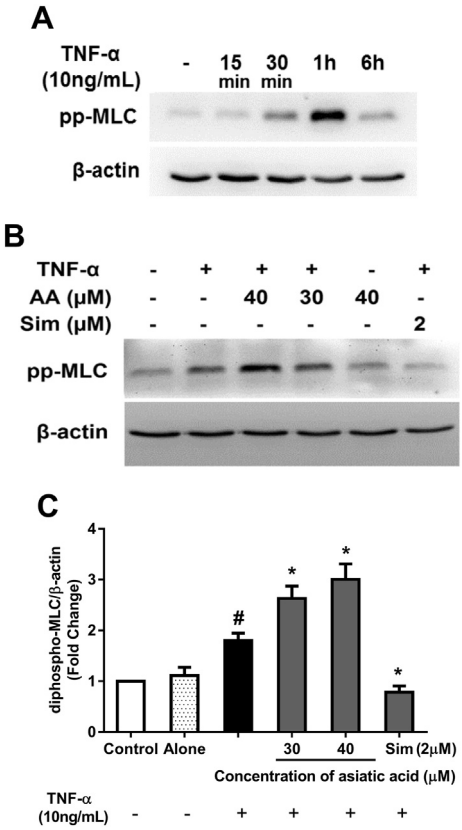

Fig. 4. Asiatic acid augments TNF-α-induced increased MLC diphosphorylation. (A) TNF-α stimulated maximal MLC diphosphorylation at 1 h. (B) A representative blot showing the effect of asiatic acid on TNF-α-induced increased MLC diphosphorylation. The cells were pre-treated with asiatic acid for 6 h and induced with TNF-α for 1 h. (C) Densitometry analysis for diphospho-MLC levels. Results are expressed as mean ± SEM of three independent experiments. AA represents asiatic acid; Sim represents simvastatin. # indicates $p < 0.05$ compared to control; * indicates $p < 0.05$ compared to TNF-α-stimulated group.

to the remaining pellet and incubated for 1 h on ice. This was then kept as F-actin fraction. The levels of F and G actin in cells were quantified using western blot analysis where actin standards were run along with each blot. The results were expressed as F to G-actin ratios.

2.5. In vitro vascular permeability assay

The permeability assay was performed using *in vitro* vascular permeability assay kits (Milipore, MA, USA) as previously described [22]. Briefly, cell culture inserts of 1 μm pore size were coated with collagen solution for 1 h. Then, HAECs were seeded into the inserts (2×10^5 cells/insert) and allowed to grow for 3 days. The bottom plate wells were filled with 500 μL of endothelial cell medium. At the end of treatment, all media was removed and 150 μL of 2000 kDa fluorescein isothiocyanate-conjugated dextran (FITC-dextran) was added into each insert. After 20 min, 100 μL of media was collected from the bottom well and transferred to a black 96-well plate. The fluorescence intensity was measured at excitation and emission wavelengths of 485 nm and 535 nm, respectively using a fluorescence microplate reader (Infinite M200, TECAN, Männedorf, Switzerland).

2.6. Immunofluorescence staining

Immunostaining was performed according to the procedure described previously [23]. HAECs were seeded onto collagen-coated 22 mm coverslips (3×10^5 cells/coverslip) and grown for 4–6 days to reach confluence. After treatment, HAECs were immediately fixed in 3.7% paraformaldehyde for 20 min and permeabilized with 0.25% Triton X-100 for 15 min. Then, the cells were blocked with 2% bovine serum albumin (BSA) for 30 min and incubated overnight at 4 °C with various primary antibodies: anti-phospho-MLC 2 (Thr18/Ser19) (1:300 dilution), anti-VE-cadherin (1:400 dilution), anti-β-catenin (1:600 dilution), anti-ZO-1 (1:500 dilution). Next, the cells were incubated with Alexa Fluor 488-conjugated secondary antibody (1:1000 dilution) for 2 h. The coverslips were then mounted with Prolong Gold anti fade agent. 5 fields per coverslip were captured at 600× using a confocal laser scanning microscope (FV1000, Olympus, Japan). For each field, *Z*-stack was performed and 9–12 sections were captured over an average depth of 4 μm. All single sections were projected into a single image.

2.7. Image analysis for junctional area of VE-cadherin and β-catenin

Quantification of junctional area was performed as previously described [24]. The junctional area of VE-cadherin and β-catenin at the cell perimeters was quantified using Image J software. The areas covered by reticular, discontinuous and linear AJs at the cell periphery were selected using free hand selections and measured in pixels. The junctional areas for 10 individual cells were measured in a field. 5 random fields were quantified for each group of treatment and the data were expressed as a percentage of total cell area.

2.8. Western blot analysis

The cells were lysed with ice-cold radioimmunoprecipitation assay (RIPA) buffer at pH 8.0 (150 mM NaCl, 50 mM Tris, 1% Triton X-100, 0.5% sodium deoxycholate, 0.1% SDS). The lysate was collected and gently shaked on ice for 10 min. Then, the lysate was centrifuged at 1000 ×*g* for 10 min at 4 °C. All the samples were quantified using Pierce™ bicinchoninic acid (BCA) assay (Thermo Fisher Scientific Inc., IL, USA) to ensure equal loading of proteins. Equal amount of protein sample (40 μg) was loaded into polyacrylamide gels and sodium dodecyl sulfate-polyacrylamide gel electrophoresis (SDS-PAGE) was performed. Then, the proteins were transferred to 0.4 μm polyvinylidene difluoride (PVDF) membranes at 100 V for 150–180 min. Next, the membrane was blocked with 5% BSA for 1 h before incubated with the following primary antibodies: anti-phospho-MLC 2 (Thr18/Ser19) (1:300 dilution), anti-VE-cadherin (1:3000 dilution), anti-β-catenin (1:3000 dilution), anti-occludin (1:300 dilution) and anti-ZO-1 (1:2000 dilution). The membrane was then incubated with anti-rabbit HRP-conjugated secondary antibody in TBST (1:5000 dilution) for 1.5 h. β-actin was used as a loading control. WesternBright™ Sirius western blotting detection kit (Advansta, CA, USA) was used to develop chemiluminescent signals of the blot.

2.9. Subcellular fractionation

The cell lysate was separated into membrane, cytosolic, nucleur and cytoskeleton fractions using ProteoExtract Subcellular Proteome Extraction kit (Milipore, MA, USA) according to the manufacturer's protocol with some modifications. Briefly, the cells were trypsinized and collected in microcentrifuge tubes. The cell lysate was centrifuged at 9300 ×*g* at 4 °C for 10 min. The supernatant was discard and 80 μL of ice-cold extraction buffer I was immediately added to the cell pellet. The lysate was incubated on ice for 10 min with gentle shaking and centrifuged at 1000 ×*g* at 4 °C for 10 min. The supernatant was kept as cytosol fractions. Extraction buffer II was immediately added to the cell pellet and the lysate was centrifuged at 6000 ×*g* for 10 min at 4 °C. The supernatant was kept as membrane fractions. Then, extraction buffer III was added to the cell pellet and the tubes were spun at 6800 ×*g*. The supernatant, known as nuclear fractions, was stored for further tests. Lastly, extraction buffer IV was added to mix the pellet and the residual was labeled as cytoskeleton fractions. All the fractions were stored at

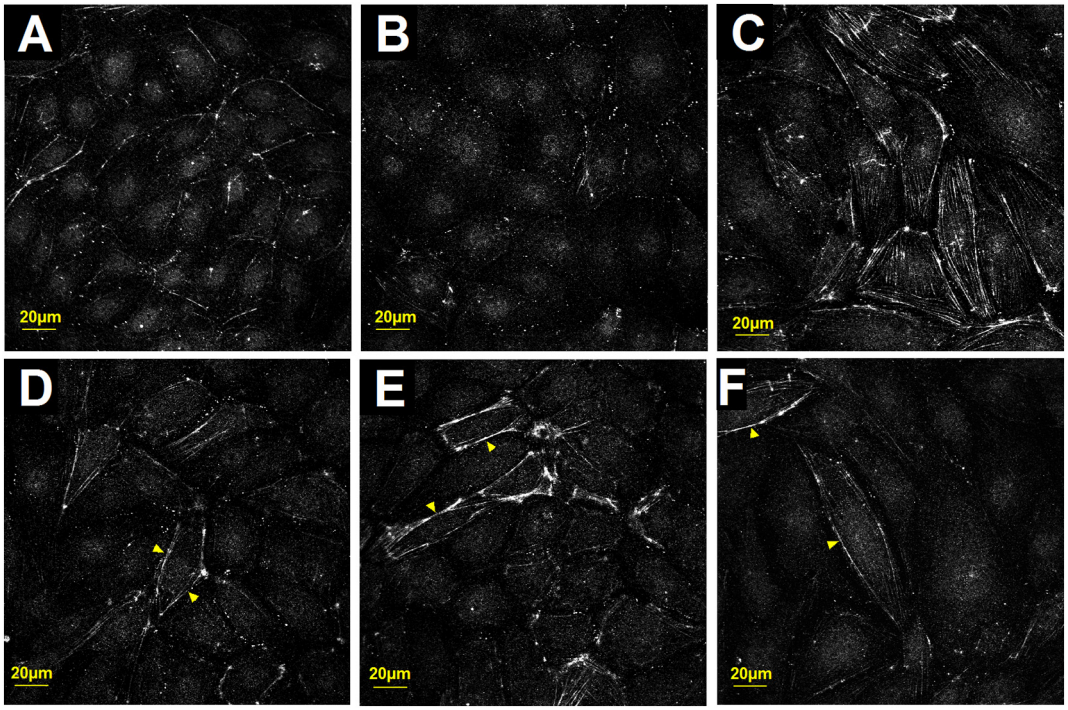

Fig. 5. Asiatic acid impedes TNF-α-induced diphospho-MLC redistribution. (A–F) Representative confocal images showing immunostaining of diphospho-MLC. HAECs were pre-treated with asiatic acid for 6 h and challenged with TNF-α for 1 h. (A) Control HAECs showed low MLC diphosphorylation levels. (B) The cells incubated with 40 μM of asiatic acid alone possessed similar diphospho-MLC distribution as the control group. (C) TNF-α increased MLC diphosphorylation at 1 h and the diphospho-MLC filaments were mainly localized at the cell center. The cells pretreated with asiatic acid at (D) 30 μM and (E) 40 μM showed localization of diphospho-MLC at cell periphery (*yellow arrowheads*). (F) The cells pretreated with simvastatin. (Bar = 20 μm). (For interpretation of the references to colour in this figure legend, the reader is referred to the web version of this article.)

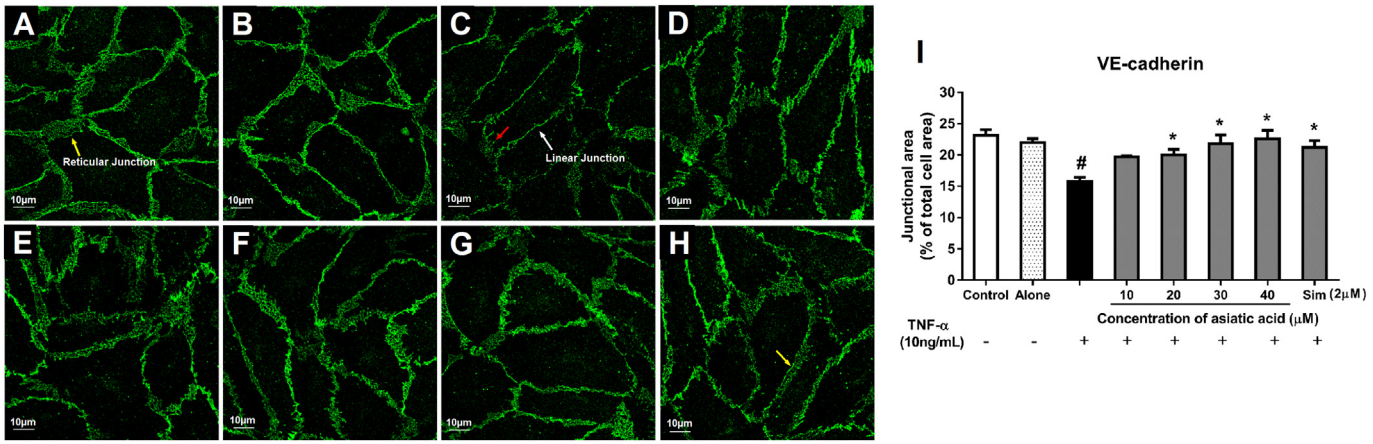

Fig. 6. Asiatic acid prevents TNF-α-induced structural remodeling of VE-cadherin. (A–H) Representative confocal images showing VE-cadherin immunostaining. (A) Control HAECs possessed thick reticular adherens junctions (*yellow arrows*). (B) Cell monolayers were incubated with 40 μM of asiatic acid alone. (C) TNF-α disrupted reticular junctions and stimulated formation of linear (*white arrows*) and discontinuous junctions (*red arrows*). The cells were pretreated with asiatic acid at (D) 10 μM, (E) 20 μM, (F) 30 μM and (G) 40 μM before induced with TNF-α. (H) Cells were pretreated with simvastatin for 24 h followed by TNF-α stimulation. (I) The junctional areas occupied by VE-cadherin. Alone, 40 μM of asiatic acid alone; Sim, simvastatin. # indicates $p < 0.05$ compared to control; * indicates $p < 0.05$ compared to TNF-α. (For interpretation of the references to colour in this figure legend, the reader is referred to the web version of this article.)

−80 °C before western blot analysis was performed.

2.10. Statistical analysis

All the data were expressed as mean ± standard error of mean (SEM). Data analysis was performed using SPSS statistical software. The data were analyzed using one-way analysis of variance (ANOVA) followed by Dunnett's test and the level of significance difference was determined at $p < 0.05$.

3. Results

3.1. Asiatic acid inhibits TNF-α-induced F-actin rearrangement

In confluent HAECs, F-actin was predominantly found along the cell periphery, forming cortical actin rings (Fig. 1A). No large intercellular gaps were observed. HAECs treated with 40 μM of asiatic acid alone showed similar F-actin distribution and cell morphology as non-stimulated cells (Fig. 1B). Upon stimulation with TNF-α, the peripheral dense F-actin filaments rearranged to form abundant stress fibers,

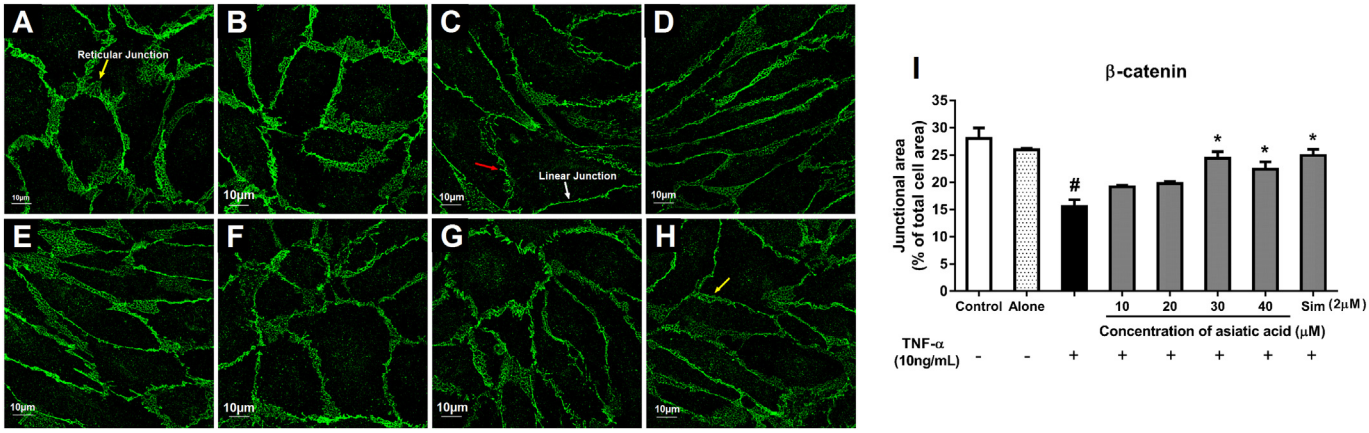

Fig. 7. Asiatic acid prevents β-catenin structural reorganization triggered by TNF-α. (A–H) Representative confocal images showing β-catenin immunostaining. (A) β-catenin formed thick reticular structure in confluent HAECs (*yellow arrows*). (B) Cell monolayers were incubated with 40 μM of asiatic acid alone. (C) TNF-α caused reticular junctions to reorganize and form linear (*white arrows*) and discontinuous AJs (*red arrows*). The cells were pretreated with asiatic acid at (D) 10 μM, (E) 20 μM, (F) 30 μM and (G) 40 μM before induced with TNF-α. (H) The cells were pretreated with simvastatin for 24 h followed by TNF-α stimulation. (I) The junctional areas occupied by β-catenin. Alone, 40 μM of asiatic acid alone; Sim, simvastatin. # indicates $p < 0.05$ compared to control; * indicates $p < 0.05$ compared to TNF-α. (For interpretation of the references to colour in this figure legend, the reader is referred to the web version of this article.)

which spanned across the cytoplasm (Fig. 1C). TNF-α also caused cell elongation and intercellular gap formation. Pretreatment of asiatic acid at 30 and 40 μM partially attenuated stress fiber formation stimulated by TNF-α as the stress fibers were not abolished completely (Fig. 1F and G). Most of the F-actin filaments were localized along the cell borders (Fig. 1F and G). However, prominent peripheral F-actin staining was not observed in the cells pretreated with 10 and 20 μM of asiatic acid (Fig. 1D and E). Simvastatin, the positive control drug, significantly suppressed TNF-α-induced increased stress fiber formation (Fig. 1H). In summary, asiatic acid prevents TNF-α-induced F-actin redistribution by preserving the peripheral F-actin filaments and partially inhibiting stress fiber formation.

3.2. Asiatic acid does not reduce TNF-α-induced increased F-actin polymerization

To investigate whether the inhibitory effect of asiatic acid on TNF-α-induced F-actin rearrangement correlates with alteration in F-actin polymerization, F/G-actin ratio was measured to indicate the degree of actin polymerization in cells. Asiatic acid alone did not alter the basal F/G-actin ratio (Fig. 2). TNF-α significantly increased F/G-actin ratio to 152.7 ± 14.8% of control ($p < 0.05$). However, 10–30 μM of asiatic acid did not suppress the TNF-α-induced increased F/G-actin ratio. Surprisingly, 40 μM of asiatic acid further augmented the increased F/G-actin ratio to 213.3 ± 15.0% of control ($p < 0.05$) (Fig. 2). Simvastatin significantly reduced the elevated F/G-actin ratio to 91.75 ± 5.6% of control ($p < 0.05$), a level which is comparable to the basal F/G-actin ratio.

3.3. Asiatic acid stabilizes F-actin filaments along the cell periphery

Next, we examined how asiatic acid preserves peripheral F-actin filaments. Cytochalasin D, an actin depolymerizing agent, significantly disrupted F-actin distribution seen in non-stimulated HAECs. In cytochalasin D-treated cells, the cortical F-actin structure was abolished and majority of the F-actin staining was condensed near the perinuclear regions (Fig. 3B). 20–40 μM of asiatic acid prevented cytochalasin D-induced disruption of F-actin filaments by retaining the peripheral F-actin filaments (Fig. 3C, D and E). These results suggest that asiatic acid may stabilize the F-actin filaments along the cell periphery.

3.4. Asiatic acid does not inhibit cytochalasin D-induced increased endothelial permeability

Then, we assessed whether asiatic acid exhibits its barrier protective effect through actin stabilization. Cytochalasin D was used to induce an increase in endothelial permeability. Cytochalasin D has been reported to increase endothelial permeability through depolymerization of actin filaments [25]. In this study, cytochalasin D significantly caused increased permeability to 722.2 ± 7.6% of control ($p < 0.05$) (Fig. 3F). However, asiatic acid did not attenuate the increased permeability elicited by cytochalasin D (Fig. 3F). On the other hand, simvastatin significantly reduced cytochalasin D-induced increased permeability to 230.7 ± 23.0% of control ($p < 0.05$). In summary, asiatic acid does not protect against cytochalasin D-induced endothelial barrier disruption by stabilizing actin.

3.5. Asiatic acid enhances TNF-α-induced increased MLC diphosphorylation

Next, MLC diphosphorylation levels at both Thr18 and Ser19 sites were examined using western blot analysis. 10 ng/mL of TNF-α stimulated maximal MLC diphosphorylation in HAECs at 1 h, and the increased diphosphorylation level was not sustained up to 6 h (Fig. 4A). Thus, we chose 1 h of induction period for TNF-α in the subsequent experiment where the effect of asiatic acid on TNF-α-induced increased MLC diphosphorylation was evaluated. TNF-α significantly elevated MLC diphosphorylation to 1.8 ± 0.1 fold of control at 1 h ($p < 0.05$) (Fig. 4B and C). Interestingly, 30 and 40 μM of asiatic acid further augmented TNF-α-induced increased MLC diphosphorylation to 2.6 ± 0.2 and 3 ± 0.3 folds, respectively ($p < 0.05$) (Fig. 4B and C). As oppose to asiatic acid, simvastatin significantly reduced the increased MLC diphosphorylation to 0.8 ± 0.1 fold of control ($p < 0.05$).

3.6. Asiatic acid prevents TNF-α-induced redistribution of diphospho-MLC

Non-stimulated HAECs possessed low levels of MLC diphosphorylation and the diphospho-MLC filaments were mainly distributed along the cell borders (Fig. 5A). TNF-α increased MLC diphosphorylation and triggered a dramatic redistribution of diphospho-MLC filaments from the cell periphery to the cytoplasm after 1 h (Fig. 5C). These diphospho-MLC filaments were found traversing across the cell body. 30 and 40 μM of asiatic acid prevented TNF-α-induced

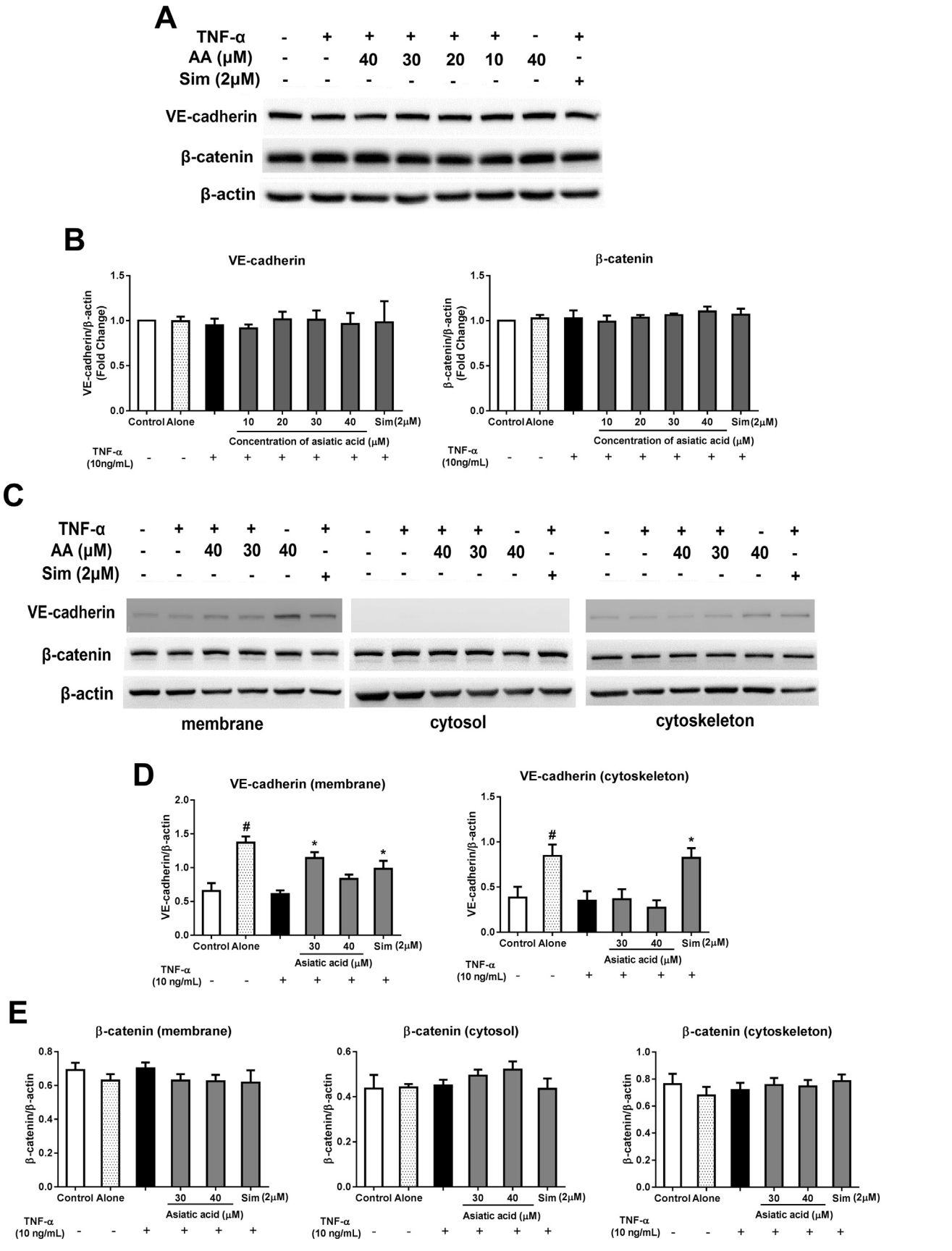

(caption on next page)

Fig. 8. Asiatic acid does not alter total AJ protein expressions but increases membrane and cytoskeletal VE-cadherin. (A) Representative blots showing total protein expression of VE-cadherin and β-catenin. (B) Densitometry analysis for total protein expression of VE-cadherin and β-catenin. Data are shown as fold changes compared to the control group and are expressed as mean ± SEM of three independent experiments. (C) Representative blots showing VE-cadherin and β-catenin expressions in membrane, cytosol and cytoskeleton fractions. (D) Densitometry analysis for VE-cadherin expressions in membrane and cytoskeleton fractions. (E) Densitometry analysis for β-catenin expressions in membrane, cytosol and cytoskeleton fractions. The values shown are mean ± SEM for three independent experiments. AA, asiatic acid; Alone, 40 μM of asiatic acid alone; Sim, simvastatin. # indicates $p < 0.05$ compared to control; * indicates $p < 0.05$ compared to TNF-α.

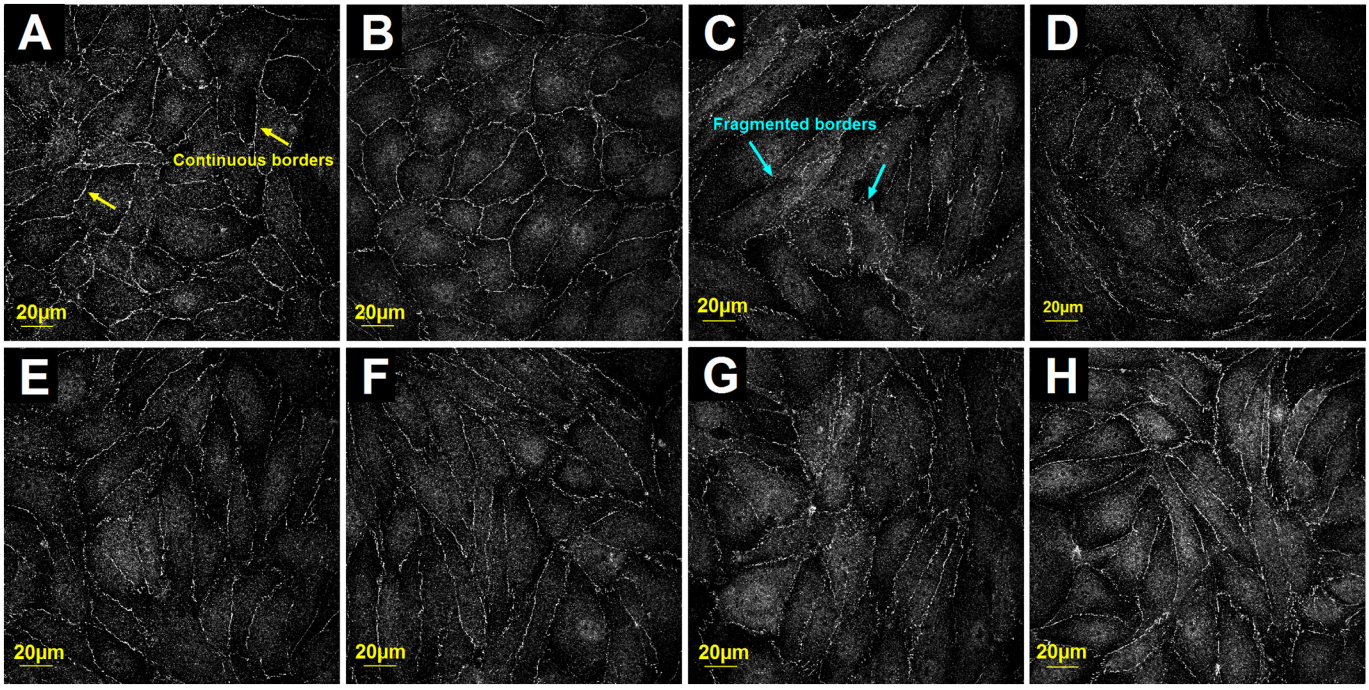

Fig. 9. Asiatic acid inhibits TNF-α-induced disassembly of ZO-1. (A-H) Representative confocal images showing ZO-1 immunostaining. (A) Control HAECs showed continuous ZO-1 staining along cell perimeters (*yellow arrows*). (B) Cell monolayers were incubated with 40 μM of asiatic acid alone. (C) TNF-α stimulated loss of ZO-1 signals from cell-cell junctions (*blue arrows*). HAECs were pretreated with asiatic acid at (D) 10 μM, (E) 20 μM, (F) 30 μM and (G) 40 μM before induced with TNF-α. (H) The cells were pretreated with simvastatin for 24 h followed by stimulation with TNF-α. (Bar = 20 μm). (For interpretation of the references to colour in this figure legend, the reader is referred to the web version of this article.)

diphospho-MLC redistribution by localizing the diphospho-MLC filaments at the cell periphery (Fig. 5D and E). Simvastatin also localized diphospho-MLC staining at the cell boundaries (Fig. 5F). These data indicate that asiatic acid may also stabilize peripheral diphospho-MLC, in addition to actin stabilization.

3.7. Asiatic acid maintains reticular adherens junctions along the cell borders

VE-cadherin and catenins form distinct subsets of adherens junctions including reticular, linear and discontinuous junctions in human umbilical vein endothelial cells (HUVECs), and these structures are highly restricted to primary endothelial cells, but not endothelial cell lines and epithelial cells [24, 26]. Here, we report that VE-cadherin and β-catenin formed reticular junctions (Fig. 6A and 7A, *yellow arrows*) and distributed continuously along the cell borders in confluent HAECs. The reticular junctions occupied significant areas at cell-cell overlapping regions and extended into the cytoplasm of adjacent endothelial cells (Fig. 6A and 7A, *yellow arrows*). A few linear junctions were also observed at the cell borders. Quantification of the junctional area showed that the junctional areas covered by VE-cadherin and β-catenin were 23.1 ± 0.9 and 28.0 ± 2.0% of total cell area, respectively (Fig. 6I and 7I).

Upon TNF-α stimulation, the reticular structure seen in non-stimulated HAECs was disrupted and majority of the cell borders were replaced with linear junctions (Fig. 6C and 7C, *white arrows*). Several discontinuous junctions were also noticed (Fig. 7C, *red arrows*). It is also worth to mention that TNF-α did not fragment the continuous VE-cadherin and β-catenin staining along the cell borders (Fig. 6C and 7C), even though most of the reticular junctions were disrupted. The linearization of reticular junctions caused by TNF-α was occurred concomitant with a reduction in the junctional area of VE-cadherin and β-catenin to 15.8 ± 0.6% (Fig. 6I) and 15.5 ± 1.3% (Fig. 7I), respectively.

Asiatic acid prevented TNF-α-induced structural reorganization of VE-cadherin and β-catenin. Reticular junctions were preserved along the cell perimeter in cells pretreated with 20, 30 and 40 μM of asiatic acid (Figs. 6E, F, G and 7E, F, G). Quantification analysis revealed that 20, 30 and 40 μM of asiatic acid significantly increased TNF-α-reduced junctional area of VE-cadherin to 20.0 ± 0.9, 21.8 ± 1.4 and 22.6 ± 1.4%, respectively ($p < 0.05$) (Fig. 6I). Furthermore, 30 and 40 μM of asiatic acid also significantly elevated the junctional area of β-catenin to 24.4 ± 1.2 and 22.4 ± 1.3%, respectively ($p < 0.05$) (Fig. 7I). Simvastatin also preserved reticular junctions (Figs. 6H and 7H, *yellow arrows*) and enhanced the junctional area of VE-cadherin and β-catenin (Figs. 6I and 7I). Taken together, asiatic acid protects against TNF-α-induced structural reorganization of adherens junctions by maintaining reticular junctions at the cell borders.

3.8. Asiatic acid affects neither total protein expressions nor subcellular distribution of AJ

In contrast to the AJ structural reorganization observed upon TNF-α stimulation, TNF-α did not alter total protein expression of VE-cadherin

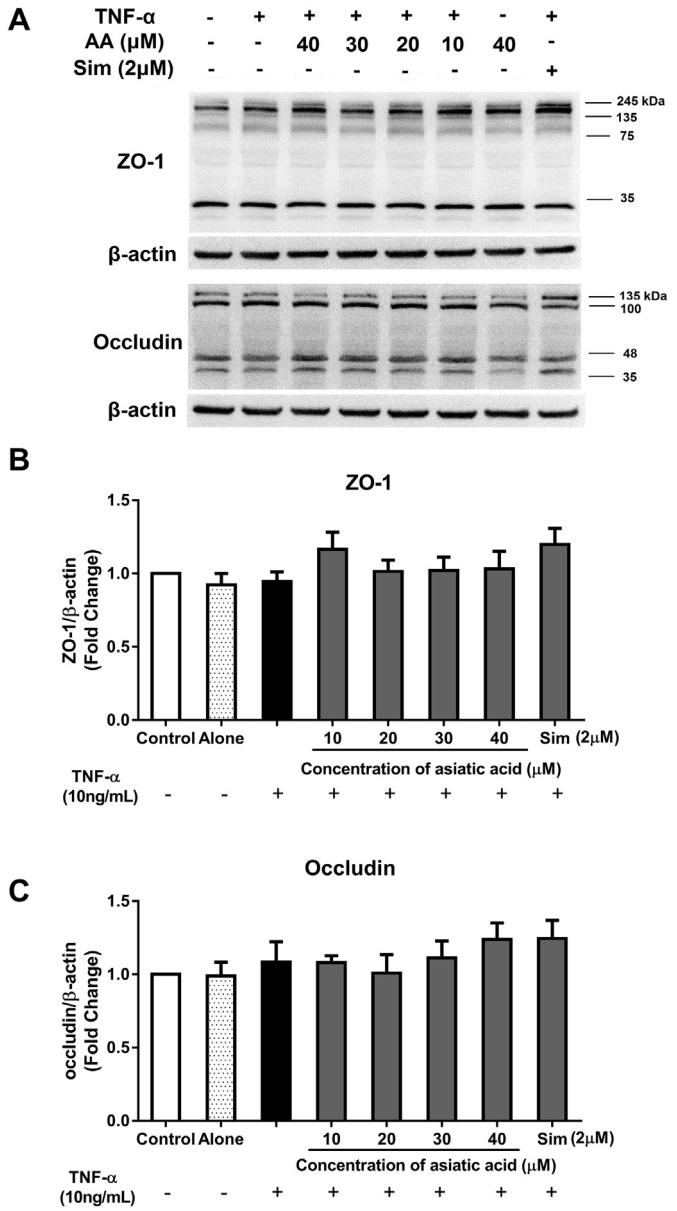

Fig. 10. Asiatic acid does not affect total ZO-1 and occludin expressions. (A) Representative blots showing total protein expression of ZO-1 and occludin. The predicted molecular weight for ZO-1 is ~225 kDa. A low molecular weight band at ~35 kDa was also detected. The predicted molecular weight of occludin is 69 kDa. However, two major occludin bands were detected at ~100–135 kDa and two more lower molecular weight bands were also detected at ~35–48 kDa. (B) Densitometry analysis for total ZO-1 expression. The analysis was done with the ZO-1 bands at ~225 kDa. (C) Densitometry analysis for total occludin expression. The analysis was done with the two major occludin bands at ~ 100–135 kDa. Data are shown as fold changes compared to the control group and expressed as mean ± SEM of three independent experiments. AA, asiatic acid; Alone, 40 μM of asiatic acid alone; Sim, simvastatin.

and β-catenin in HAECs (Fig. 8B). Then, we examined whether TNF-α and asiatic acid could affect the distribution of VE-cadherin and β-catenin in different subcellular compartments. In cells treated with TNF-α, no redistribution of VE-cadherin and β-catenin between membrane, cytosol and cytoskeleton fractions was observed (Fig. 8C, D and E). Interestingly, 30 μM of asiatic acid significantly increased membrane VE-cadherin expression in TNF-α-treated HAECs ($p < 0.05$), despite the fact that TNF-α did not alter membrane VE-cadherin contents (Fig. 8D). Besides, 40 μM of asiatic acid alone significantly elevated both membrane and cytoskeletal VE-cadherin expressions ($p < 0.05$) (Fig. 8D), implying that asiatic acid alone not only increases VE-cadherin contents at the cell membrane but also enhances the association between VE-cadherin and the cytoskeleton. Simvastatin also significantly increased both membrane and cytoskeletal VE-cadherin expression upon TNF-α stimulation ($p < 0.05$).

3.9. Asiatic acid prevents TNF-α-induced tight junction disassembly

ZO-1 formed a nearly continuous line along the cell perimeter in confluent HAECs (Fig. 9A, *yellow arrows*). TNF-α induced loss of ZO-1 signals and caused discontinuous ZO-1 staining along the cell perimeter (Fig. 9C, *blue arrows*). Notably, the ZO-1 staining did not completely disappear from the cell borders but appeared much more fragmentary compared to non-stimulated HAECs. 20, 30 and 40 μM of asiatic acid prevented TNF-α-induced ZO-1 disassembly (Fig. 9E, F and G). Besides, simvastatin also maintained continuous ZO-1 staining along the cell perimeter upon TNF-α induction (Fig. 9H). In summary, asiatic acid protects against TNF-α-induced disassembly of tight junctions.

3.10. Asiatic acid abrogates TNF-α-induced redistribution of ZO-1 and occludin

TNF-α did not affect the total content of ZO-1 and occludin (Fig. 10). Hence, we further examined intracellular distribution of ZO-1 and occludin in membrane, cytosol and cytoskeleton fractions to investigate how asiatic acid protects against tight junction disassembly triggered by TNF-α. The ZO-1 expression was detected in the membrane and cytosol only but not the cytoskeleton (Fig. 11A). TNF-α triggered internalization of membrane ZO-1 to cytoplasm (Fig. 11B). This was in line with the confocal images showing that ZO-1 was disrupted and redistributed from the cell borders upon TNF-α stimulation (Fig. 9C). 30 and 40 μM of asiatic acid significantly prevented TNF-α-induced ZO-1 redistribution (Fig. 11B). Simvastatin also significantly inhibited the internalization of ZO-1 from membrane to cytosol (Fig. 11B).

In contrast to ZO-1, TNF-α did not change membrane occludin expression including both high (100–135 kDa) and low (35–48 kDa) molecular weight occludin (Fig. 11C). For the cytosolic and cytoskeleton fractions, densitometry analysis was performed for occludin bands at ~69 kDa. Interestingly, TNF-α caused redistribution of cytosolic occludin to the cytoskeleton and this was inhibited by asiatic acid at both 30 and 40 μM (Fig. 11D). Simvastatin also significantly abrogated occludin redistribution triggered by TNF-α. Taken together, asiatic acid hinders TNF-α-induced intracellular redistribution of tight junctions.

4. Discussion

Asiatic acid, one of the major triterpenes isolated from *C. asiatica*, has recently garnered the interest of scientists as it has been demonstrated to possess a wide range of biological activities. Asiatic acid has been shown to improve the lipid profile of hyperlipidemic rats [15] and restores hemodynamic abnormalities in metabolic syndrome rats [27]. We previously reported that asiatic acid suppresses increased endothelial permeability and increased vascular adhesion molecule-1 expressions induced by TNF-α [22]. Asiaticoside, the glycoside of asiatic acid, has also been shown to attenuate TNF-α-induced HAEC hyperpermeability and F-actin rearrangement [23]. Yet, the mechanisms underlying the barrier protective effect of asiatic acid have never been extensively elucidated. In the present study, we showed that asiatic acid partially attenuated TNF-α-induced F-actin rearrangement and stabilized peripheral F-actin filaments. However, asiatic acid did not improve endothelial barrier dysfunction through actin stabilization. Asiatic acid also enhanced TNF-α-induced increased MLC diphosphorylation and localized diphospho-MLC filaments along the cell periphery. Moreover, the anti-hyperpermeability effect of asiatic acid was found concomitant with both the maintenance of reticular AJs and enhancement of TJ assembly.

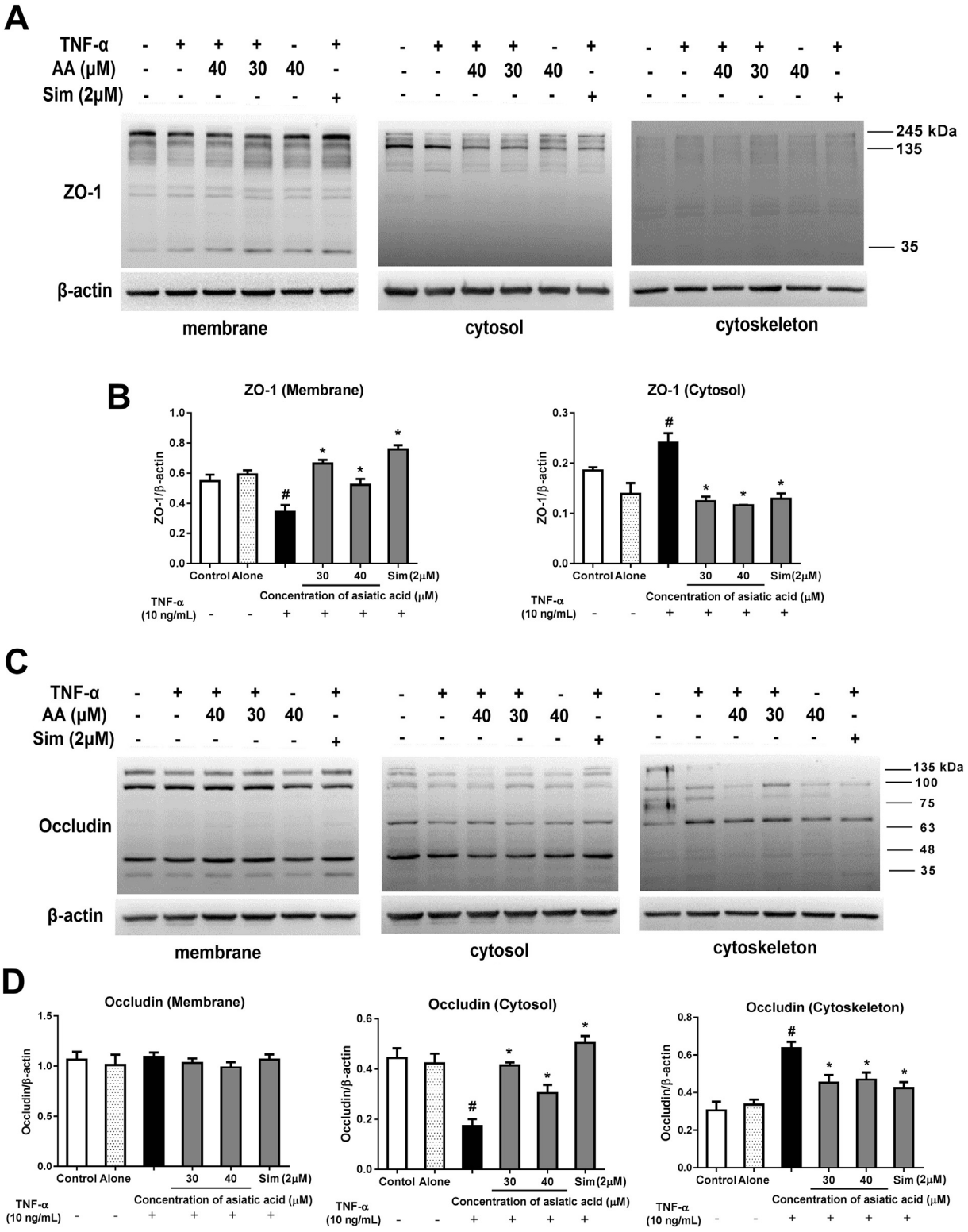

Fig. 11. Asiatic acid prevents TNF-α-induced redistribution of TJ proteins among subcellular fractions. (A) Representative blots showing ZO-1 protein expressions in the membrane, cytosol and cytoskeleton fractions of HAECs. 30 and 40 μM of asiatic acid prevented redistribution of membrane ZO-1 to the cytosol stimulated by TNF-α (B) Densitometry analysis for membrane and cytosolic ZO-1 was performed. (C) Representative blots showing occludin protein expressions in the membrane, cytosol and cytoskeleton fractions of HAECs. 30 and 40 μM of asiatic acid abrogated TNF-α-induced redistribution of cytosolic occludin to the cytoskeleton. (D) Densitometry analysis for membrane, cytosolic and cytoskeletal occludin was performed. The major occludin bands at ~69kDa were analyzed. Data are shown as mean ± SEM of three independent experiments. AA, asiatic acid; Alone, 40 μM of asiatic acid alone; Sim, simvastatin. # indicates $p < 0.05$ compared to control; * indicates $p < 0.05$ compared to TNF-α.

Actin cytoskeleton is an important determinant of endothelial barrier function and proper regulation of the actin cytoskeleton is required to maintain the integrity of endothelial barrier [28]. The enhancement of peripheral cortical actin network has been associated with barrier protective effects of several agents including sphingosine-1-phosphate [29] and a standardized hawthorn extract known as WS®1442 [30]. We demonstrated that asiatic acid preserved peripheral F-actin filaments and partially suppressed TNF-α-induced stress fiber formation (Fig. 1). Researchers have reported that both preservation of peripheral F-actin filaments and inhibition of stress fiber formation are important for endothelial barrier stabilization [31]. However, asiatic acid failed to suppress the increased F-actin polymerization stimulated by TNF-α (Fig. 2). As such, asiatic acid may preserve peripheral F-actin filaments by acting through a mechanism other than reducing F-actin polymerization. Indeed, we showed that asiatic acid prevented cytochalasin D-induced F-actin disassembly (Fig. 3). Cytochalasin D, an actin depolymerization agent, acts as capping proteins that bind the barbed end of actin filaments and inhibits addition or dissociation of actin to occur at the barbed end [32]. Hence, we suggest that asiatic acid preserves the F-actin organization through stabilization of peripheral F-actin. Yet, actin stabilization is not essential for asiatic acid to protect against cytochalasin D-induced endothelial barrier disruption, as asiatic acid failed to attenuate the increased permeability caused by cytochalasin D (Fig. 3).

An increase in MLC phosphorylation is crucial for the generation of acto-myosin contractile forces [3]. The general consensus is that inflammatory mediators such as vascular endothelial growth factor and histamine cause increased MLC phosphorylation, which is accompanied with stress fiber formation that pull the junction proteins apart and in turn, disrupts the endothelial barrier [5]. However, an earlier study suggested that the endothelial barrier integrity is not solely determined by the overall reduction of MLC diphosphorylation, but rather, it is dependent on the intracellular distribution of the diphospho-MLC [31]. Our data clearly demonstrated that asiatic acid inhibited TNF-α-induced diphospho-MLC redistribution by localizing peripheral diphospho-MLC (Fig. 5), on top of the enhancement of TNF-α-stimulated increased MLC diphosphorylation levels (Fig. 4). Sphingosine-1-phosphate (S1P), a well-known barrier protective molecule released by platelets, has been demonstrated to confine diphospho-MLC staining at sites of cortical actin ring and elevate MLC diphosphorylation levels [33].

As the actin cytoskeleton is not involved in the barrier enhancement effect of asiatic acid, we then investigated the roles of intercellular junctions. VE-cadherin and β-catenin form AJ complexes at cell-cell contact areas to regulate the paracellular permeability [34]. Several mechanisms have previously been proposed to disrupt the endothelial junction complexes, including decreased protein expressions [35], internalization [36] and phosphorylation of junction proteins [37], which eventually results in increased endothelial permeability. We demonstrated that TNF-α disrupted reticular junctions in HAECs and this was found in parallel with neither decreased AJ protein expressions nor their intracellular redistribution. Our data is in line with previous reports showing that TNF-α causes structural reorganization of AJs in HUVECs, independent of reduced AJ contents [38] and intracellular relocalization of AJs [24].

A highlight of the present study is that asiatic acid protected against TNF-α-induced disruption of reticular AJs by enhancing the junctional areas covered by VE-cadherin and β-catenin (Figs. 6 and 7). Several barrier protective molecules have been reported to possess their effects through promoting increased junctional areas. For example, oxidized 1-palmitoyl-2-arachidonoyl-sn-glycero-3-phosphocholine (OxPAPC), an oxidized phospholipid, has been demonstrated to improve endothelial barrier function by increasing peripheral junctional area covered by AJs [39]. Besides, S1P has also been reported to expand the size of AJs at cell-cell contact area and the increased junction size is independent of actomyosin-driven contractile force [40]. Furthermore, our data also suggest that structural integrity maintenance of AJs plays a relatively more important role than alteration of AJ protein expressions in the prevention of TNF-α-induced endothelial barrier disruption, in view of the data demonstrating that AJ protein expressions were unaltered upon TNF-α challenge.

Occludin, claudins and junction adhesion molecules (JAM) seal the endothelial barrier by forming TJs with cytoplasmic ZO-1. AJs is believed to initiate junction assembly at cell-cell contact areas and maintain the endothelial barrier, whereas TJs further enhance tightness of the barrier integrity particularly in brain microvasculature which possesses extremely low basal permeability [41]. In contrast to changes seen in AJs, our findings suggest that TJ redistribution, rather than their structural reorganization, might underlie the mechanism by which TNF-α induces TJ disassembly in artery endothelial cells (Figs. 9 and 11). In HUVECs, TNF-α has been reported to cause ZO-1 redistribution from cell-cell junctions, without affecting the total expression of ZO-1 [42]. Furthermore, we failed to demonstrate immunostaining of occludin in the present study and this might be due to low occludin expressions seen in HAECs. Cheung et al. (2012) reported that occludin displays weak fluorescence signals in HAECs [43]. Eiselein et al. (2007) also failed to demonstrate localization of occludin at the borders of HAECs [44].

The present study also provides clear evidence supporting that asiatic acid protected against TNF-α-induced disassembly of TJs by preventing intracellular redistribution of ZO-1 and occludin (Fig. 11). It has been reported that several barrier protective agents maintain barrier integrity through enhancement of TJ complex formation. S1P promotes the assembly of TJ complexes by promoting ZO-1 and claudin-5 redistribution to the cell boundaries through a cortactin-dependent pathway [45, 46]. FTY720 (*S*)-phosphonate, a novel analogue of S1P, increases peripheral ZO-1 distribution, albeit that silencing of ZO-1 only partially modulates barrier protective effect of FTY720 (*S*)-phosphonate [47].

In conclusion, this study provides better understanding on how TNF-α disrupts junction complexes in HAECs. Besides, the present findings unveil the mechanism by which asiatic acid possess its endothelial barrier protective effect, where the maintenance of AJ structures and promotion of TJ assembly play a pivotal role. Asiatic acid also stabilizes both actin and diphospho-MLC, albeit this is not important for its barrier-stabilizing effect. This supports a potential therapeutic use of asiatic acid in the prevention of early pre-lesional stage of atherosclerosis, which involves endothelial hyperpermeability as an initiating step.

Conflict of interest

The authors declare that there is no conflict of interest.

Author contributions

Fong performed the experiments, analyzed the data and wrote the manuscript. Ng performed some of the experiments and edited the manuscript. Yong and Nazrul edited and finalized the manuscript. Zuraini received a grant for this project and supervised this study.

Acknowledgements

This study was funded by the Ministry of Higher Education, Malaysia under Fundamental Research Grant Scheme (FRGS/1/2015/SKK06/UPM/02/4). The authors would also like to acknowledge the late Dr. Zuraini Ahmad for her significant contributions in this study. Dr. Zuraini wrote the proposal, provided guidance to and supervised Fong in completing this study.

References

[1] S.D. Funk, A. Yurdagul Jr., A.W. Orr, Hyperglycemia and endothelial dysfunction in atherosclerosis: lessons from type 1 diabetes, Int. J. Vasc. Med. 2012 (2012) 569654.

[2] C.S. Stancu, L. Toma, A.V. Sima, Dual role of lipoproteins in endothelial cell dysfunction in atherosclerosis, Cell Tissue Res. 349 (2012) 433–446.

[3] N.V. Bogatcheva, A.D. Verin, The role of cytoskeleton in the regulation of vascular endothelial barrier function, Microvasc. Res. 76 (2008) 202–207.

[4] N. Prasain, T. Stevens, The actin cytoskeleton in endothelial cell phenotypes, Microvasc. Res. 77 (2009) 53–63.

[5] Q. Shen, M.H. Wu, S.Y. Yuan, Endothelial contractile cytoskeleton and microvascular permeability, Cell Health Cytoskeleton 2009 (2009) 43–50.

[6] P. Hashim, Centella asiatica in food and beverage applications and its potential antioxidant and neuroprotective effect, Int. Food Res. J. 18 (2011) 1215–1222.

[7] Assessment Report on *Centella asiatica* (L.) Urban, Herba, In, European Medicines Agency:1–44.

[8] M.R. Cesarone, G. Belcaro, A.N. Nicolaides, et al., Increase in echogenicity of echolucent carotid plaques after treatment with total triterpenic fraction of Centella asiatica: a prospective, placebo-controlled, randomized trial, Angiology 52 (Suppl. 2) (2001) S19–S25.

[9] L. Incandela, G. Belcaro, A.N. Nicolaides, et al., Modification of the echogenicity of femoral plaques after treatment with total triterpenic fraction of Centella asiatica: a prospective, randomized, placebo-controlled trial, Angiology 52 (Suppl. 2) (2001) S69–S73.

[10] G. Belcaro, E. Ippolito, M. Dugall, et al., Pycnogenol(R) and *Centella asiatica* in the management of asymptomatic atherosclerosis progression, Int. Angiol. 34 (2015) 150–157.

[11] G. Belcaro, M. Dugall, M. Hosoi, et al., Pycnogenol(R) and Centella Asiatica for asymptomatic atherosclerosis progression, Int. Angiol. 33 (2014) 20–26.

[12] G. Belcaro, U. Cornelli, Variations in echogenicity in carotid and femoral atherosclerotic plaques with Pycnogenol + Centella Asiatica supplementation, Int. J. Angiol. 26 (2017) 95–101.

[13] M.T. De Sanctis, G. Belcaro, L. Incandela, et al., Treatment of edema and increased capillary filtration in venous hypertension with total triterpenic fraction of Centella asiatica: a clinical, prospective, placebo-controlled, randomized, dose-ranging trial, Angiology 52 (Suppl. 2) (2001) S55–S59.

[14] G.V. Belcaro, R. Grimaldi, G. Guidi, Improvement of capillary permeability in patients with venous hypertension after treatment with TTFCA, Angiology 41 (1990) 533–540.

[15] V. Ramachandran, R. Saravanan, P. Senthilraja, Antidiabetic and antihyperlipidemic activity of asiatic acid in diabetic rats, role of HMG CoA: in vivo and in silico approaches, Phytomedicine 21 (2014) 225–232.

[16] K.J. Yun, J.Y. Kim, J.B. Kim, et al., Inhibition of LPS-induced NO and PGE2 production by asiatic acid via NF-kappa B inactivation in RAW 264.7 macrophages: possible involvement of the IKK and MAPK pathways, Int. Immunopharmacol. 8 (2008) 431–441.

[17] S.S. Huang, C.S. Chiu, H.J. Chen, et al., Antinociceptive activities and the mechanisms of anti-inflammation of asiatic acid in mice, Evid. Based Complement. Alternat. Med. 2011 (2011) 895857.

[18] V. Ramachandran, R. Saravanan, Asiatic acid prevents lipid peroxidation and improves antioxidant status in rats with streptozotocin-induced diabetes, J. Funct. Foods 5 (2013) 1077–1087.

[19] W. Sun, G. Xu, X. Guo, et al., Protective effects of asiatic acid in a spontaneous type 2 diabetic mouse model, Mol. Med. Rep. 16 (2017) 1333–1339.

[20] P. Maneesai, S. Bunbupha, U. Kukongviriyapan, et al., Effect of asiatic acid on the Ang II-AT1R-NADPH oxidase-NF-kappaB pathway in renovascular hypertensive rats, Naunyn Schmiedeberg's Arch. Pharmacol. 390 (2017) 1073–1083.

[21] S. Bunbupha, P. Pakdeechote, U. Kukongviriyapan, et al., Asiatic acid reduces blood pressure by enhancing nitric oxide bioavailability with modulation of eNOS and p47phox expression in L-NAME-induced hypertensive rats, Phytother. Res. 28 (2014) 1506–1512.

[22] L.Y. Fong, C.T. Ng, Z.L. Cheok, et al., Barrier protective effect of asiatic acid in TNF-alpha-induced activation of human aortic endothelial cells, Phytomedicine 23 (2016) 191–199.

[23] L.Y. Fong, C.T. Ng, Z.A. Zakaria, et al., Asiaticoside inhibits TNF-α-induced endothelial Hyperpermeability of human aortic endothelial cells, Phytother. Res. 29 (10) (2015) 1501–1508.

[24] L. Fernandez-Martin, B. Marcos-Ramiro, C.L. Bigarella, et al., Crosstalk between reticular adherens junctions and platelet endothelial cell adhesion molecule-1 regulates endothelial barrier function, Arterioscler. Thromb. Vasc. Biol. 32 (2012) e90–102.

[25] J. Waschke, F.E. Curry, R.H. Adamson, et al., Regulation of actin dynamics is critical for endothelial barrier functions, American journal of physiology, Heart Circ. Physiol. 288 (2005) H1296–H1305.

[26] J. Millan, R.J. Cain, N. Reglero-Real, et al., Adherens junctions connect stress fibres between adjacent endothelial cells, BMC Biol. 8 (2010) 11.

[27] P. Pakdeechote, S. Bunbupha, U. Kukongviriyapan, et al., Asiatic acid alleviates hemodynamic and metabolic alterations via restoring eNOS/iNOS expression, oxidative stress, and inflammation in diet-induced metabolic syndrome rats, Nutrients 6 (2014) 355–370.

[28] H. Schnittler, M. Taha, M.O. Schnittler, et al., Actin filament dynamics and endothelial cell junctions: the Ying and Yang between stabilization and motion, Cell Tissue Res. 355 (2014) 529–543.

[29] X. Sun, Y. Shikata, L. Wang, et al., Enhanced interaction between focal adhesion and adherens junction proteins: involvement in sphingosine 1-phosphate-induced endothelial barrier enhancement, Microvasc. Res. 77 (2009) 304–313.

[30] M.F. Bubik, E.A. Willer, P. Bihari, et al., A novel approach to prevent endothelial hyperpermeability: the Crataegus extract WS(R) 1442 targets the cAMP/Rap1 pathway, J. Mol. Cell. Cardiol. 52 (2012) 196–205.

[31] N.V. Bogatcheva, M.A. Zemskova, C. Poirier, et al., The suppression of myosin light chain (MLC) phosphorylation during the response to lipopolysaccharide (LPS): beneficial or detrimental to endothelial barrier? J. Cell. Physiol. 226 (2011) 3132–3146.

[32] J.A. Cooper, Effects of cytochalasin and phalloidin on actin, J. Cell Biol. 105 (1987) 1473–1478.

[33] S.M. Dudek, J.R. Jacobson, E.T. Chiang, et al., Pulmonary endothelial cell barrier enhancement by sphingosine 1-phosphate: roles for cortactin and myosin light chain kinase, J. Biol. Chem. 279 (2004) 24692–24700.

[34] I.H. Sarelius, A.J. Glading, Control of vascular permeability by adhesion molecules, Tissue Barriers 3 (2015) e985954.

[35] K.D. Rochfort, P.M. Cummins, Cytokine-mediated dysregulation of zonula occludens-1 properties in human brain microvascular endothelium, Microvasc. Res. 100 (2015) 48–53.

[36] J. Gavard, J.S. Gutkind, VEGF controls endothelial-cell permeability by promoting the beta-arrestin-dependent endocytosis of VE-cadherin, Nat. Cell Biol. 8 (2006) 1223–1234.

[37] W. Shen, S. Li, S.H. Chung, et al., Tyrosine phosphorylation of VE-cadherin and claudin-5 is associated with TGF-beta1-induced permeability of centrally derived vascular endothelium, Eur. J. Cell Biol. 90 (2011) 323–332.

[38] J. Hu, Z. Zhang, H. Xie, et al., Serine protease inhibitor A3K protects rabbit corneal endothelium from barrier function disruption induced by TNF-alpha, Invest. Ophthalmol. Vis. Sci. 54 (2013) 5400–5407.

[39] A.A. Birukova, N. Zebda, P. Fu, et al., Association between adherens junctions and tight junctions via Rap1 promotes barrier protective effects of oxidized phospholipids, J. Cell. Physiol. 226 (2011) 2052–2062.

[40] Z. Liu, J.L. Tan, D.M. Cohen, et al., Mechanical tugging force regulates the size of cell-cell junctions, Proc. Natl. Acad. Sci. U. S. A. 107 (2010) 9944–9949.

[41] Y. Komarova, A.B. Malik, Regulation of endothelial permeability via paracellular and transcellular transport pathways, Annu. Rev. Physiol. 72 (2010) 463–493.

[42] J.A. McKenzie, A.J. Ridley, Roles of rho/ROCK and MLCK in TNF-alpha-induced changes in endothelial morphology and permeability, J. Cell. Physiol. 213 (2007) 221–228.

[43] T.M. Cheung, M.P. Ganatra, E.B. Peters, et al., Effect of cellular senescence on the albumin permeability of blood-derived endothelial cells, American journal of physiology, Heart Circ. Physiol. 303 (2012) H1374–H1383.

[44] L. Eiselein, D.W. Wilson, M.W. Lame, et al., Lipolysis products from triglyceride-rich lipoproteins increase endothelial permeability, perturb zonula occludens-1 and F-actin, and induce apoptosis, American journal of physiology, Heart Circ. Physiol. 292 (2007) H2745–H2753.

[45] J.F. Lee, Q. Zeng, H. Ozaki, et al., Dual roles of tight junction-associated protein, zonula occludens-1, in sphingosine 1-phosphate-mediated endothelial chemotaxis and barrier integrity, J. Biol. Chem. 281 (2006) 29190–29200.

[46] P. Belvitch, S.M. Dudek, Role of FAK in S1P-regulated endothelial permeability, Microvasc. Res. 83 (2012) 22–30.

[47] L. Wang, R. Bittman, J.G. Garcia, et al., Junctional complex and focal adhesion rearrangement mediates pulmonary endothelial barrier enhancement by FTY720 S-phosphonate, Microvasc. Res. 99 (2015) 102–109.